Size dependence of exciton-phonon coupling in sol-gel ZnMgO powders

C. H. Chia, J. N. Chen, T. C. Han, J. W. Chiou, Y. C. Lin, W. L. Hsu, and W. C. Chou

Citation: Journal of Applied Physics **109**, 063526 (2011); doi: 10.1063/1.3563574
View online: http://dx.doi.org/10.1063/1.3563574
View Table of Contents: http://scitation.aip.org/content/aip/journal/jap/109/6?ver=pdfcov
Published by the AIP Publishing

Size dependence of exciton-phonon coupling in sol-gel ZnMgO powders

C. H. Chia,[1,a] J. N. Chen,[1] T. C. Han,[1] J. W. Chiou,[1] Y. C. Lin,[2] W. L. Hsu,[2] and W. C. Chou[2]
[1]*Department of Applied Physics, National University of Kaohsiung, Kaohsiung 81148, Taiwan*
[2]*Department of Electrophysics, National Chiao Tung University, Hsin-Chu 30010, Taiwan*

(Received 28 January 2011; accepted 6 February 2011; published online 23 March 2011)

We found that the exciton-phonon coupling in the $Zn_{1-x}Mg_xO$ powders ($0.01 \leqq x \leqq 0.07$) is greatly influenced by the crystalline-size. Two well-resolved photoluminescence (PL) bands due to recombination of free exciton and its longitudinal optical (LO)-phonon replicas enable us to analyze the relative intensities among free excitons, one-LO-phonon replicas, and two-LO-phonon replicas. As crystalline size increases, a larger enhancement of the PL-intensity ratio of a free exciton to its LO-phonon replicas was found compared to that of two LO-phonon replica to one-LO-phonon replica. © *2011 American Institute of Physics*. [doi:10.1063/1.3563574]

I. INTRODUCTION

There is a large potential for the development of light-emitting devices operating in the UV-to-deep-UV spectral range using $Zn_{1-x}Mg_xO$ ternary alloy semiconductors as an active layer in optoelectronic devices.[1,2] In our previous letter, we reported the biexcitonic emissions of sol-gel $Zn_{1-x}Mg_xO$ powders.[3] It was found that the emission of a longitudinal-optical (LO) phonon sideband is obvious in the sol-gel $Zn_{1-x}Mg_xO$ powders at high temperature (T). As excitation density increases, the exciton-phonon interaction competed with the inelastic exciton-exciton scattering process, which is an important transition for stimulated emission in ZnO-based nanostructures. It is well known that the exciton-phonon coupling (EPC) effect is significant in ZnO-based materials, which possess large ionicity and polarity. It affects the stability of excitons at high T. Therefore the EPC is an important issue to ZnO-based materials.

The photoluminescence (PL) properties of ZnO-based nanostructures have been intensively studied due to their potential application in the nanoscale optoelectronic devices.[4–9] It was found that the EPC can differ significantly from the bulk counterpart to the nanostructure systems. Among the literature, several interpretations were given for the enhancement of EPC in ZnO nanostructures, such as free exciton reabsorption,[4] imperfections in the crystal,[5–8] and lattice heating.[9] In particular, the room-temperature (RT) PL of ZnO-based nanostructures was characterized by a single emission band due to free excitons (FX) and LO phonon-assisted excitonic recombinations.[4–8] No well-resolved emission band was detected because the studies only limited to samples with small size.

We systematically studied the EPC of $Zn_{1-x}Mg_xO$ powders with a size from nano- to micrometer. The separation of FX-emission band and its LO-phonon sideband allows us to investigate the crystalline-size (d_{size}) dependence of EPC. We found that the d_{size} of the powders greatly influences the emission peak energy and integrated intensity of phonon-assisted excitonic transitions.

[a] Author to whom all correspondence should be addressed. Electronic mail: chchia@nuk.edu.tw.

II. EXPERIMENT

The $Zn_{1-x}Mg_xO$ powders were grown from aqueous solution prepared using zinc nitrate hexahydrate [$Zn(NO_3)_2{\cdot}6H_2O$] and magnesium nitrate hexahydrate [$Mg(NO_3)_2{\cdot}6H_2O$] as the starting materials, de-ionized water as the solvent, and citric acid ($C_6H_8O_7$) as the stabilizer. The precursor solutions were mixed thoroughly until the formation of sols. The sols were preheated in a furnace at 120 °C for 12 h to evaporate the solvent and successively at 600 °C for 2 h to remove the organic residuals. The powders obtained from the dried sols were then post-annealed at calcination-temperature (T_C) = 600, 800, and 1000 °C for 2 h in ambient air. The Mg content x in the samples is $0.01 \leqq x \leqq 0.07$, determined by the exciton energy obtained from low-T reflection spectra, according to Ref. 10. From the results of x-ray diffraction measurement (x-ray beam $CuK_\alpha = 0.154$ nm), no signal of MgO phase was detected from the samples. The d_{size} of the $Zn_{1-x}Mg_xO$ powders was confirmed by field emission scanning electron microscope (FESEM).

The PL spectra were measured by a 32-cm-long monochromator and a charge-coupled device camera. The samples were excited by 266-nm line of neodymium-doped yttrium aluminum garnet (Nd:YAG) laser. The pulsed laser has a pulse width of 10 ns and a repetition rate of 20 Hz. The excitation-power was kept as low as 20 W/cm^2 to avoid high-excitation effect of excitons. A closed cycle refrigerator was used to perform the T-dependent measurement.

III. RESULTS AND DISCUSSION

The FESEM images of the samples ($0.01 \leqq x \leqq 0.07$) with T_C = 600, 800, and 1000 °C are shown in Figs. 1(a) to 1(f), respectively. Regardless of Mg concentrations, the d_{size} of the powders depends crucially on T_C. As T_C increases from 600 to 1000 °C, the d_{size} of the powders increases. The average d_{size} of the samples annealed at 600, 800, and 1000 °C are 0.2, 0.5, and 0.9 μm, respectively, as shown in Fig. 2(a). The corresponding RT-PL spectra of these samples are shown in Fig. 2(b). A single emission band was observed for the samples with $d_{size} \sim 0.2$ μm, whereas two well-resolved emission bands were observed in the samples with

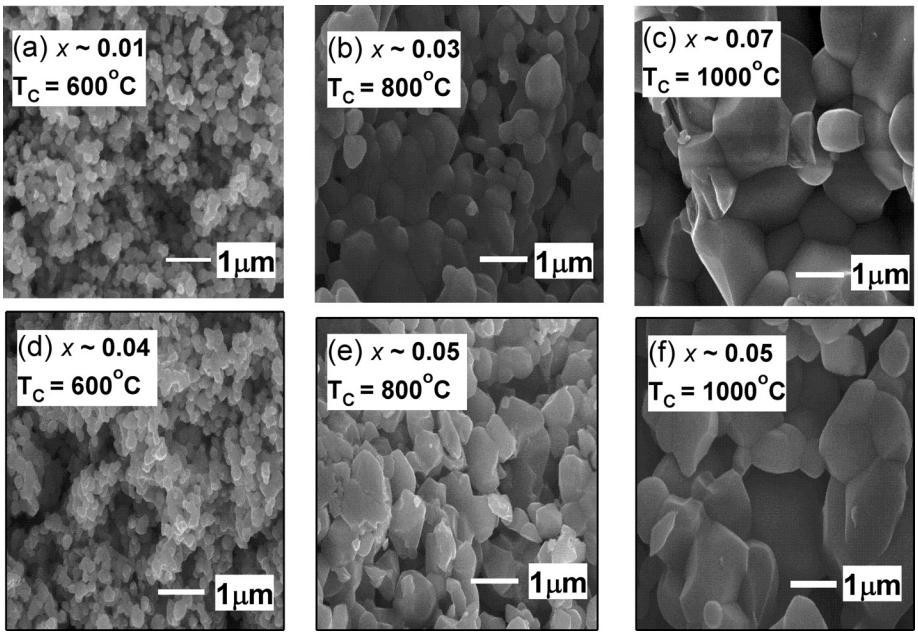

FIG. 1. The field emission scanning electron microscope image of $Zn_{1-x}Mg_xO$ powders (a) $x \sim 0.01$, $T_C = 600\,^{\circ}C$; (b) $x \sim 0.03$, $T_C = 800\,^{\circ}C$; (c) $x \sim 0.07$, $T_C = 1000\,^{\circ}C$; (d) $x \sim 0.04$, $T_C = 600\,^{\circ}C$; (e) $x \sim 0.05$, $T_C = 800\,^{\circ}C$; (f) $x \sim 0.05$, $T_C = 1000\,^{\circ}C$.

$d_{size} \sim 0.5$ and 0.9 μm. With comparison to the RT-reflectance spectra (not shown), the high-energy emission bands can be attributable to the radiative recombination of *FX*, denoted as open squares. The energetic separations of the low-energy bands and the *FX* bands are 82 and 110 meV for the samples with $d_{size} \sim 0.5$ and 0.9 μm, respectively. The *FX* emissions of the samples with $d_{size} \sim 0.2$ μm are weak, and the PL are dominated by emission bands with peak energies about 65 meV lower than the *FX* energies determined from RT-reflectance measurement.

To clarify the origin of low-energy PL bands of the samples, we performed the *T*-dependent PL measurement. In Figs. 3(a)–3(c), we show the typical *T*-dependent PL spectra of the $Zn_{1-x}Mg_xO$ powders ($0.04 \leqq x \leqq 0.05$) with $d_{size} \sim 0.2$, 0.5, and 0.9 μm, respectively. The PL spectra are dominated by radiative recombination of excitons localized at alloy potential fluctuation at low *T*, judging from the Stoke's shift between the PL peak energy and the *FX* energy obtained from low-*T* reflectance measurement. At 100 K, the PL peak energies blueshift because of delocalization of excitons. After 100 K, as excitons become mobile, new emissions attributable to LO phonon-sidebands of *FX* (denote as *FX-1LO*) emerge in the PL spectra of all of the samples. At 100 K, The energetic separations between these *FX-1LO* lines and the *FX* lines are about 56 meV. The value matches well with the theoretical energetic separation calculated from $\Delta E = E_{LO} - 1.5k_BT$ (Ref. 11) with $E_{LO} = 72$ meV.[12] The two-LO-phonon assisted excitonic transitions (*FX-2LO*) appear in the PL bands after 200 K. This could be interpreted as being due to the thermalization effect of *FX*. At high *T*, *FX*'s with large wave vector *k* increase, and the simultaneous emission of photons and LO phonons becomes a most efficient *FX* annihilation process.[13] Therefore we can assign the low-energy PL bands to a combined *FX-1LO* and *FX-2LO* transition in the samples. It is well-known that the Fröhlich interaction plays a major role in EPC in highly polar ZnO materials.[14] However, the Fröhlich interaction is

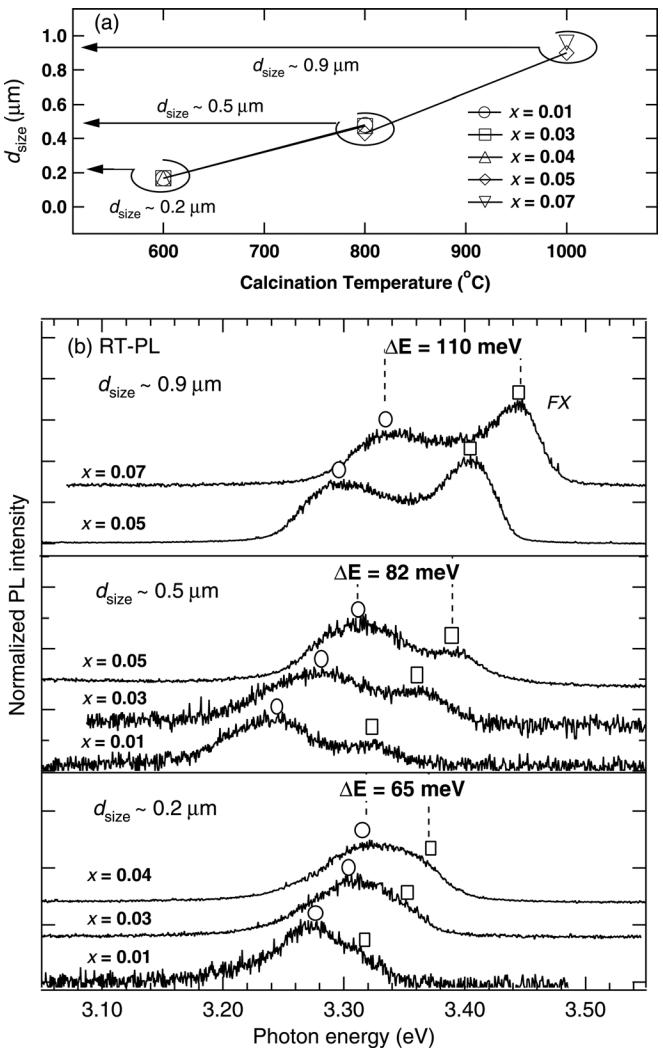

FIG. 2. (a) The d_{size} of $Zn_{1-x}Mg_xO$ powders ($0.01 \leqq x \leqq 0.07$) as a function of T_C. (b) The corresponding RT-PL of the $Zn_{1-x}Mg_xO$ powders. The open squares and solid circles represent the peak energy positions of *FX* and LO-phonon sidebands, respectively. The average d_{size}'s and the Mg concentrations are also given at the left-hand side.

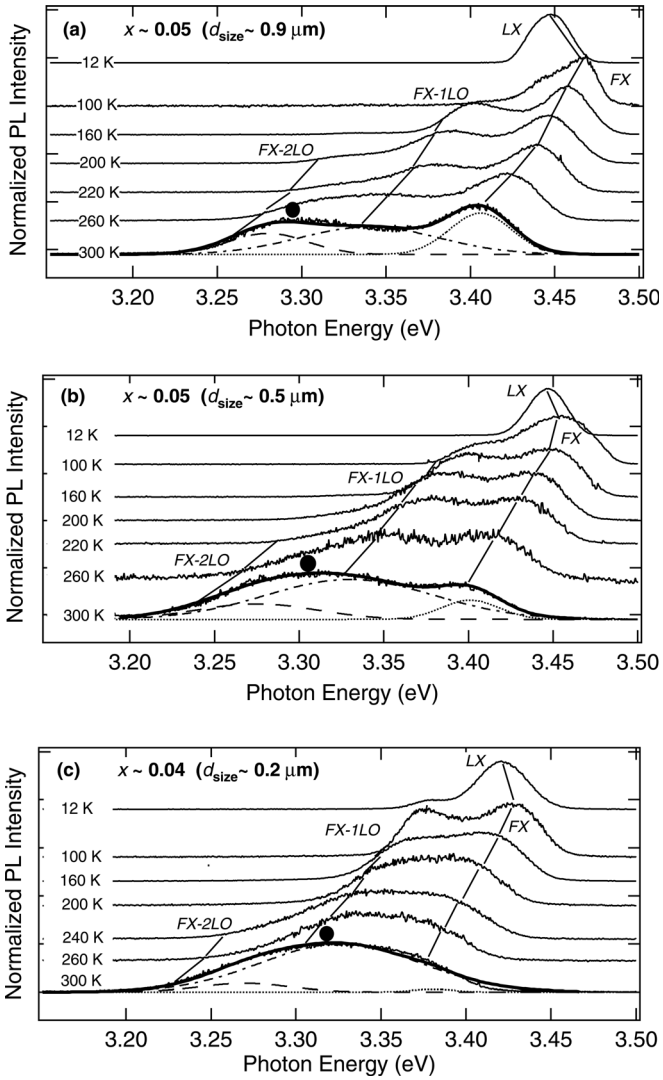

FIG. 3. (a) *T*-dependent PL spectra for $Zn_{0.95}Mg_{0.05}O$ powders ($d_{size} \sim 0.9$ μm). (b) *T*-dependent PL spectra for $Zn_{0.95}Mg_{0.05}O$ powders ($d_{size} \sim 0.5$ μm). (c) *T*-dependent PL spectra for $Zn_{0.96}Mg_{0.04}O$ powders ($d_{size} \sim 0.2$ μm). Lines are given to guide the evolution of the PL band of *FX*, *FX-LO*, and *FX-2LO* as a function of *T*. The solid circles indicate the peak position of the combined 1LO- and 2LO-phonon replicas. Bolded solid curves on the PL spectra of 300 K are the fitting results. The dotted, dot-dashed, and dashed curves represent the contributions due to *FX*, *FX-1LO*, and *FX-2LO*, respectively.

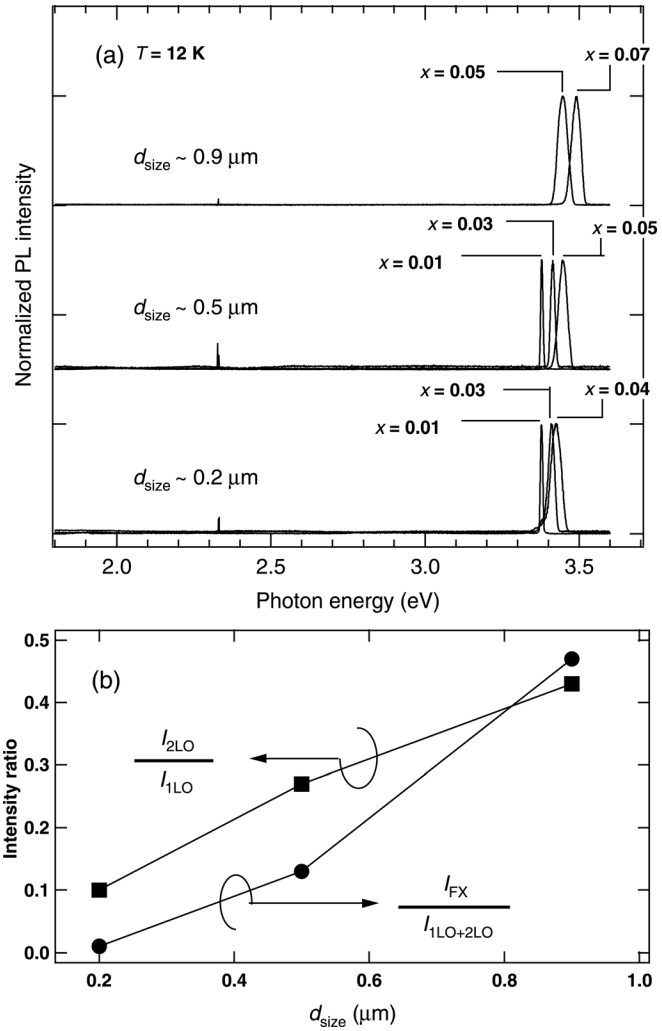

FIG. 4. (a) The low-*T* PL spectra of $Zn_{1-x}Mg_xO$ powders. The PL spectra are dominated by radiative recombination of localized excitons and the deep level emission is negligible. (b) The PL-intensity ratio I_{2LO}/I_{1LO} (solid squares) and $I_{FX}/I_{1LO+2LO}$ (solid circles).

extremely small in a perfect crystal due to the parity conservation, which results in a weak exciton-LO phonon coupling.[5,9] At low *T*, because the lateral extension of exciton wave function is limited by the localization,[15] the EPC is expected to be small according to the Huang–Rhys model,[16] which states that the EPC decreases as the separation between electrons and holes decreases. Therefore phonon sidebands are negligible at low *T*. As an exciton becomes free, a strong EPC is still not expected because of parity conservation mentioned in the preceding text. The lattice heating[9] effect is unlikely under the low-excitation power (20 W/cm^2). Also, the *FX* reabsorption effect[4] can not explain the increase in *FX*-emission intensity in the large-d_{size} powder because a larger reabsorption is expected for the samples with larger d_{size}. Therefore we interpret the strong LO-phonon-assisted *FX* emission observed in the samples as being due to the crystal-imperfection in the powders.[5–8] In Fig. 4(a), we show the low-*T* PL spectra for all of the samples. The deep level emission is negligible, indicating crystal imperfection inside the powders could be excluded for consideration. Therefore we emphasize that the most decisive factor resulting in a strong LO-phonon-assisted *FX* emissions mainly stem from the surface defects.

We note that the PL-intensity ratios of *FX*, *FX-1LO,* and *FX-2LO* are significantly different among the samples with $d_{size} \sim 0.2$, 0.5, and 0.9 μm. To quantify the relative contributions of the *FX*, *FX-1LO,* and *FX-2LO* processes to the RT-PL spectra of the $Zn_{1-x}Mg_xO$ powders ($0.04 \leqq x \leqq 0.05$), the line shape of each PL band was fitted by three Gaussians that give a good approximation to the line shapes of both the *FX* and its LO phonon replica (bold solid lines in Fig. 3). The spectral positions of *FX-1LO* and *FX-2LO* are about 55 and 120 meV lower than that of *FX*. These values are smaller than the energies of one-*LO* phonon (72 meV) and two-*LO* phonons (144 meV) because of thermal distribution at RT.[11] The integrated intensity ratio of the *FX* (I_{FX}) to its LO phonon

replica ($I_{1LO+2LO}$) is shown in Fig. 4(b). The $I_{FX}/I_{1LO+2LO}$ ratio increases from 0.01 to 0.47 as d_{size} increases from 0.2 to 0.9 μm because there is a larger portion of *FX* that radiatively recombines inside the interior region than that at the proximity of surface region in the powder with larger d_{size}. We also show the integrated PL intensity-ratio I_{2LO}/I_{1LO} in Fig. 4(b). The ratio increases from 0.1 to 0.43 as d_{size} increases from 0.2 to 0.9 μm, leading to the redshift of LO-phonon-assisted *FX* emissions. The I_{2LO}/I_{1LO} ratio, which is proportional to the Huang–Rhys factor S,[16] could be an indicator for the strength of EPC. The increase in EPC with increasing d_{size} was also reported for ZnO quantum dots[17] and nanowires,[18] using Raman spectroscopy. As the d_{size} increases, the extent of excitonic wave function can spread over a larger region with longer electron-hole separation. These excitons strongly coupled with the polarization field of LO phonons at the surface region, leading to larger S.[17]

IV. CONCLUSION

In conclusion, by investigating the RT-PL of a series of $Zn_{1-x}Mg_xO$ powders ($0.01 \leqq x \leqq 0.07$), we found that the EPC effect in the powders is greatly influenced by the d_{size} but irrelevant to the Mg concentrations. Two well-resolved PL bands due to recombination of *FX* and its LO-phonon replicas enable us to study the relative intensities among *FX*, *FX-1LO,* and *FX-2LO*. As d_{size} increases, a larger enhancement of $I_{FX}/I_{1LO+2LO}$ ratio was found compared to that of I_{2LO}/I_{1LO} ratio. This implies that both ratios have to be considered when discussing the origin of RT-PL from ZnO-based nanostructures having various sizes.

ACKNOWLEDGMENTS

This research was supported by National Science Council of Taiwan under Grant No. NSC-99–2112-M-390–001-MY3.

[1]H. Tampo, H. Shibata, K. Maejima, A. Yamada, K. Matsubara, P. Fons, S. Niki, T. Tainaka, Y. Chiba, and H. Kanie, Appl. Phys. Lett. **91**, 261907 (2007).
[2]H. Zhu, C. X. Shan, B. H. Li, Z. Z. Zhang, J. Y. Zhang, B. Yao, D. Z. Shen, and X. W. Fan, J. Appl. Phys. **105**, 103508 (2009).
[3]C. H. Chia, Y. J. Lai, W. L. Hsu, T. C. Han, J. W. Chiou, Y. M. Hu, Y. C. Lin, W. C. Fan, and W. C. Chou, Appl. Phys. Lett. **96**, 191902 (2010).
[4]S. L. Chen, S. K. Lee, W. M. Chen, H. X. Dong, L. Sun, Z. H. Chen, and I. A. Buyanova, Appl. Phys. Lett. **96**, 033108 (2010).
[5]T. Voss, C. Bekeny, L. Wischmeier, H. Gafsi, S. Börner, W. Schade, A. C. Mofor, A. Bakin, and A. Waag, Appl. Phys. Lett. **89**, 182107 (2006).
[6]C. H. Ahn, S. K. Mohanta, N. E. Lee, and H. K. Cho, Appl. Phys. Lett. **94**, 261904 (2009).
[7]W. K. Hong, G. Jo, M. Choe, T. Lee, J. I. Sohn, and M. E. Welland, Appl. Phys. Lett. **94**, 043103 (2009).
[8]X. Gu, K. Huo, G. Qian, J. Fu, and P. K. Chu, Appl. Phys. Lett. **93**, 203117 (2008).
[9]Y. J. Xing, Z. H. Xi, Z. Q. Xue, X. D. Zhang, J. H. Song, R. M. Wang, J. Xu, Y. Song, S. L. Zhang, and D. P. Yu, Appl. Phys. Lett. **83**, 1689 (2003).
[10]M. Lorenz, E. M. Kaidashav, A. Rahm, Th. Nobis, J. Lenzner, G. Wagner, D. Spemann, H. Hochmuth, and M. Grudmann, Appl. Phys. Lett. **86**, 143113 (2005).
[11]C. Klingshirn, Phys. Status Solidi B **71**, 547 (1975).
[12]Ü. Özgür, Ya. I. Alivov, C. Liu, A. Teke, M. A. Reshchikov, S. Doğan, A. Avrutin, S.-J. Cho, and H. Morkoc, J. Appl. Phys. **98**, 041301 (2005).
[13]W. Shan, W. Walukiewicz, J. W. Ager III, K. M. Yu, H. B. Yuan, H. P. Xin, G. Cantwell, and J. J. Song, Appl. Phys. Lett. **86**, 191911 (2005).
[14]R. P. Wang, G. Xu, and P. Jin, Phys. Rev. B **69**, 113303 (2004).
[15]T. Makino, K. Tamura, C. H. Chia, Y. Segawa, M. Kawasaki, A. Ohtomo, and H. Koinuma, Phys. Rev. B **66**, 233305 (2002).
[16]K. Huang, and A. Rhys, Proc. R. Soc. London, Ser. A **204**, 406 (1950).
[17]R. C. Ray, Y. Low, H. M. Tsai, C. W. Pao, J. W. Chiou, S. C. Yang, F. Z. Chien, W. F. Pong, M.-H. Tsai, K. F. Lin, H. M. Cheng, W. F. Hsieh, J. F. Lee, Appl. Phys. Lett **91**, 262101 (2007).
[18]S. Nomura, and T. Kobayashi, Phys. Rev. B **45**, 1305 (1992).